

# Characterization, photocatalytic, and antibacterial activity of Ag–TiO<sub>2</sub> nanoparticles prepared by electrical arc discharge method

Mahdi Hajivaliei<sup>\*</sup>, Majid Lashkanpour

*Department of Physics, Bu-Ali Sina University, Hamedan, Iran*

*<sup>\*</sup>E-mail: mhaji65@yahoo.com*

**Received 6 December 2011**

**Received in revised form 18 March 2012**

**Accepted 20 March 2012**

---

A simple, inexpensive and one-step synthesis route of Ag-TiO<sub>2</sub> nanoparticles by arc discharge method is reported. The resulting nanoparticles were characterized using X-ray diffraction and scanning electron microscopy. X-ray diffraction patterns demonstrate dominance of rutile to anatase phase in TiO<sub>2</sub> and formation of silver metal on TiO<sub>2</sub> after arc discharge process. Scanning electron microscopy images exhibit the increase of reduced nanoparticles in 5 minutes arc duration compared with 1 minute arc duration. Photodegradation of Methyl Orange as a standard pollutant shows that the presence of silver in TiO<sub>2</sub> was found to enhance the photocatalytic activity. The high activity of silver doped TiO<sub>2</sub> is due to the enhancement of electron-hole separation by the electron trapping of silver particles. Antibacterial activities of Ag-TiO<sub>2</sub> nanoparticles were investigated at the presence of Escherichia coli bacteria.

**Keywords:** Ag-TiO<sub>2</sub> nanoparticles; Antibacterial activity; Electrical arc discharge method; Photocatalytic activity

---

## 1. INTRODUCTION

Titanium dioxide (TiO<sub>2</sub>) has attracted significant attention of researchers because of many interesting physical properties that make it suitable for a variety of applications [1, 2]. When TiO<sub>2</sub> is exposed by photon which its energy is more than TiO<sub>2</sub>'s band gap, electron is excited from valance band to conduction band, then the electron-hole pair will be created [3, 4]. This phenomenon leads to hydrophilic and photocatalytic properties of TiO<sub>2</sub>. Combination of these properties plan many applications such as solar cells [5, 6], refinement of air and water [7, 8], gas sensors [9], and self-cleaning surface [10, 11].

Nevertheless multivarious studies were achieved; many researches are performed for improvement of properties. The only disadvantage of TiO<sub>2</sub> is that its band gap lies in the near-Ultraviolet (UV) of electromagnetic spectrum: 3.2 electron volt (eV) and 3.0 eV for anatase and rutile, respectively. It is therefore, evident that any modification of the TiO<sub>2</sub>-based photocatalysts, resulting in a lowering of its band gap, is representing a breakthrough in the field [12, 13]. Efforts have been made to extend the energy absorption range of TiO<sub>2</sub> from UV to visible light or to improve further the photocatalytic activity of TiO<sub>2</sub> by adding foreign metallic elements [14–16].

For instance, Ag can serve as electron trap aiding electron-hole separation, and can also facilitate electron excitation by creating a local electric field. When Ag is deposited upon TiO<sub>2</sub>, electron of electron-hole pair is trapped by silver. During radiation, then recombination rate is decreased [17, 18]. Also, attention is paid for antibacterial properties of Ag [19, 20] such as interesting plasmonic properties in nanometric dimension, easy preparation, and low price [21]. In this study, we examined the photocatalytic degradation of the methyl orange (MO) in the aqueous

suspensions of TiO<sub>2</sub> and Ag-deposited TiO<sub>2</sub> nanoparticles under UV light irradiation in order to evaluate and distinguish the various effects of Ag deposits on the TiO<sub>2</sub> photocatalytic activity. The X-Ray Diffraction (XRD) pattern and scanning electron microscopy (SEM) images of prepared materials were taken.

## 2. EXPERIMENTAL

### 2.1. Material

TiO<sub>2</sub> powder was supplied from Gohsenol Company. The nano silver particles were made by electric arc discharge technique and then added to TiO<sub>2</sub> powder. The methyl orange, polyvinyl alcohol and monoethanol amide stearate were purchased from Merck Company. Also the E.coli bacteria are collected from Iranian National Center for Genetic.

### 2.2. Preparation of nanoparticles

The preparation system consists of two main parts: a high current DC power supply and a reactor including anode, cathode, and a micrometer which moves the anode towards the cathode. The schematic diagram of the electrical arc discharge is shown in Fig.1. A 50 ampere (A) arc current was applied between two silver electrodes. The voltage was dropped to about 20 volt (V) during the arc performance, while the current was fixed to desired value. Both anode and cathode were disk shaped silver, 1 cm diameter and 2 mm thickness, and 99.99% purity. In this arc current, which was the threshold current for discharge between silver electrodes, discharge happens only between the electrodes and there is negligible erosion for titanium electrodes.

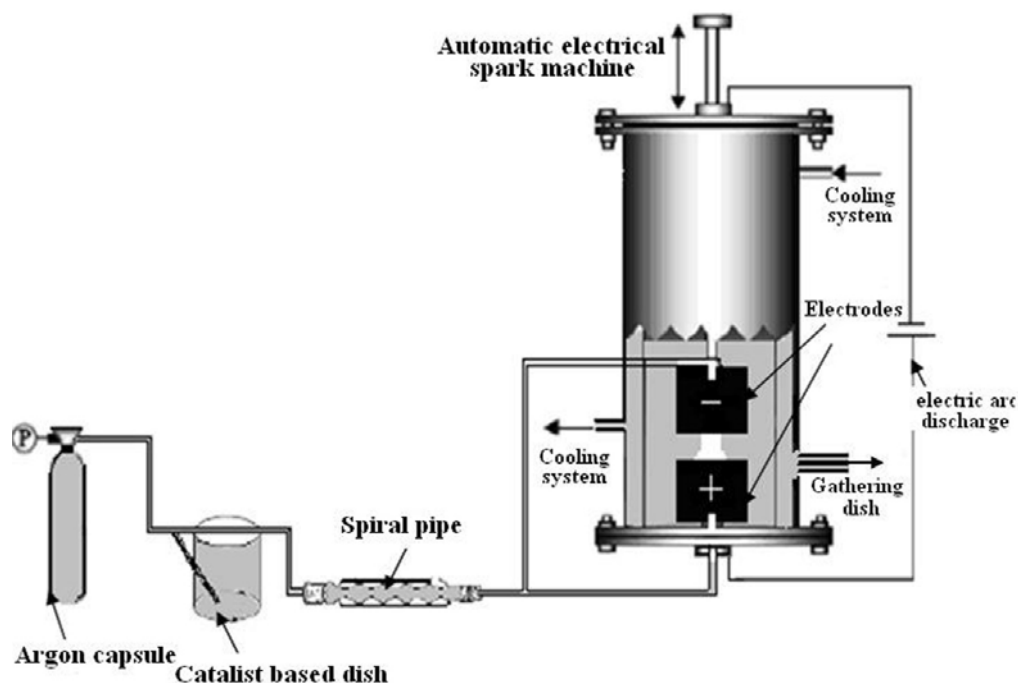


**Fig. 1.** Schematic diagram showing the arc discharge process.

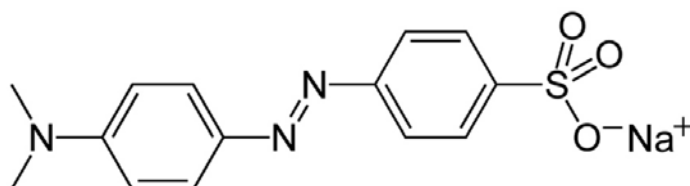
Two electrodes were connected to automatic electrical spark in suitable distance. Initially we bring the two electrodes into touch leading to a small contact cross section and thus to a high current density. When argon passes through the path with 300 mbar pressure, Ar gas transits the based catalyst (Titanium dioxide) to system's box. Hence, Ag metal is vaporized and embedded on based catalyst. External product was trapped in dish which consists of polyvinyl alcohol 10%, 40

monoethanol amide stearate 2%, and the rest is deionization water. Collected products were annealed by heater at 120 °C for 60 min. Also, products were calcined at 600 °C for 60 min, and finally it was grinded.

## 2.3. Characterization

### 2.3.1. Measurements of photocatalytic activities

To investigate the effects of silver deposition on the photocatalytic activity of TiO<sub>2</sub>, the photodegradation of MO was carried out in the TiO<sub>2</sub>, 0.1% Ag-TiO<sub>2</sub> and 0.5% Ag-TiO<sub>2</sub> nanosols under UV light irradiation, respectively. The molecular structure of MO is given in scheme 1. A 100 ml pyrex beacker was used as a batch photoreactor. The TiO<sub>2</sub> or Ag-TiO<sub>2</sub> nanosol (50 mL) containing MO (10<sup>-5</sup> mol L<sup>-1</sup>) was transferred into the photoreactor, and aerated with stirring for 30 min in the dark. The MO/nanosol was then irradiated with the lamp located above the reactor at given irradiation time intervals. The light sources, purchased from Philips Company, were 30 Watt and working in 254 nm, A1 ml-aliquot was taken from the MO/nanosol and analyzed by UV-visible absorption spectroscopy (Perkin Elmer 550ES model) to monitor the degree of the MO photodegradation.



**Scheme 1.** The molecular structure of methyl orange.

### 2.3.2. Antibacterial test

Silver nanoparticles are known for their antimicrobial properties and have been used for years in the medical field for antimicrobial applications [22, 23]. Additionally, silver has been used in water and air filtration to eliminate micro-organisms [24]. Antibacterial test was performed by Kirby-Bauer method [25] and used culture medium of Mueller-Hinton agar. All glass water and materials were sterilized in autoclave at 121°C and 1 atmosphere pressure for 30 min before experiments. In this way, 10<sup>5</sup>cfu (colony forming unit)/ml of E. coli O157 were used as the experimental bacteria and cultured on the culture medium at 37 °C for 18-24 hours then, special disks (blank disk) containing of experimental material were postured in the Petri dish of culture medium. When a material had covered on the disk, the material spreads to the agar. The solvability of considered material and its molecular size, determine the integument area. If a micro-organism is cultivated on the agar, whereas it can't grow, area of no growing is considered as zone of inhibition [26].

## 3. RESULTS AND DISCUSSION

### 3.1. XRD analysis

The X-Ray Diffraction pattern of the powder samples synthesized in different concentration are taken by ADP2000 model from Italstructure Company and shown in Fig.2. It can be seen that phase of titanium dioxide is completely rutile. After deposition of TiO<sub>2</sub> with Ag, crystal peaks (111) and (200) of silver metal appear in 2θ = 38.15 and 44.34 degrees, respectively. By increasing the silver percentage, intensity of these peaks improves and then (220) and (311) crystal peaks of silver appear in 2θ = 64.5 and 77.47degrees, respectively.

### 3.2. SEM analysis

Microscopic structure of the samples was observed by scanning electron microscopy images obtained by LEO 1455 VP model. Fig. 3a and 3b illustrate scanning electron microscopy images of Ag-TiO<sub>2</sub> nanoparticles prepared at 50A arc current with 1 and 5 minutes arc duration, respectively.

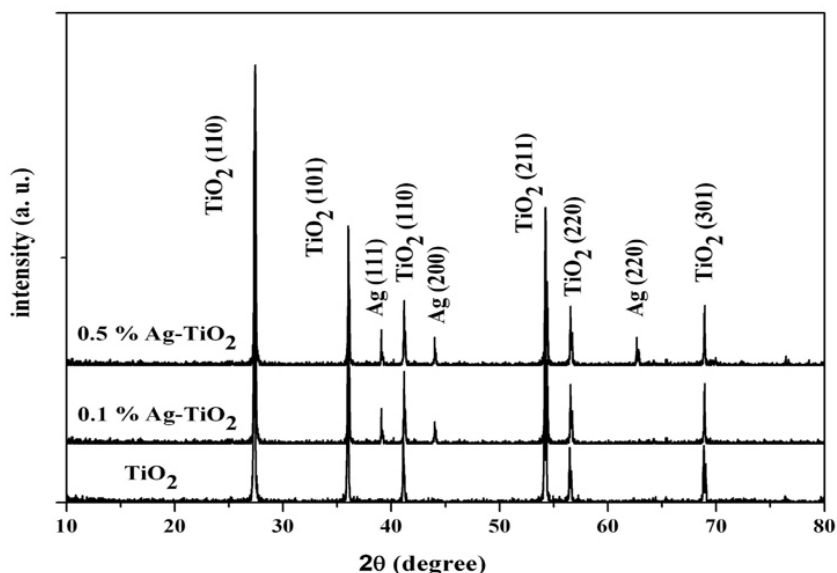


**Fig. 2.** XRD pattern of TiO<sub>2</sub>, at 0.1% Ag-TiO<sub>2</sub> and at 0.5% Ag-TiO<sub>2</sub> synthesized powder.

The amount of reduced nanoparticles at 5 minutes arc duration is much higher than the reduced nanoparticles at 1 min arc duration. The obtained size is about 90 nm in 1 min duration and is about 70 nm for 5 min duration. The amount of electrons injected from discharge zone to the solution in 5 min arc duration, is more than the injected electrons in 1 min arc duration, which resulting in more reduced nanoparticles. It was observed that the particles are nanosized and spherical.

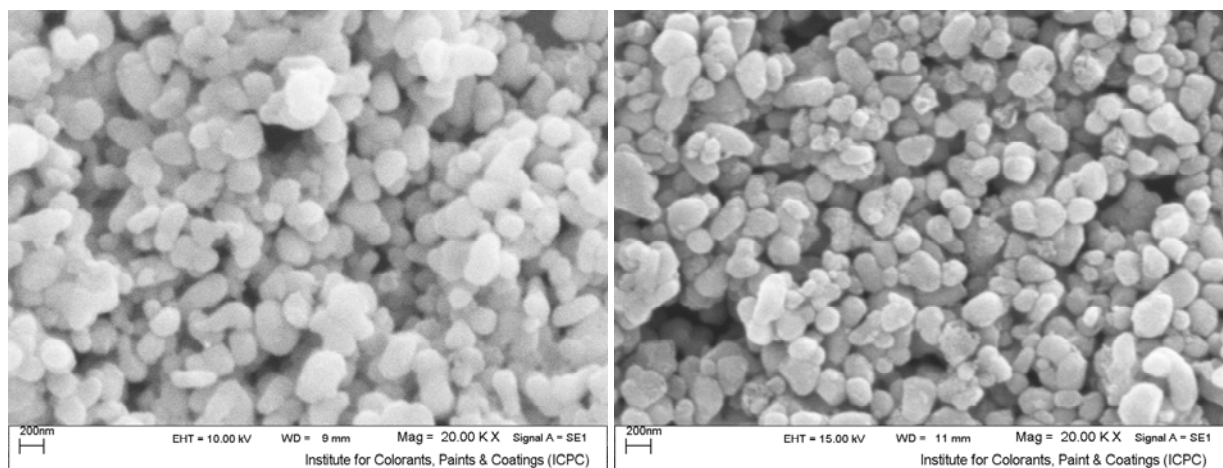


**Fig. 3.** SEM images of (a) 0.1% Ag-TiO<sub>2</sub> nanoparticles with 1 and (b) 0.5% Ag-TiO<sub>2</sub> nanoparticles 5 minutes arc durations.

### 3.3. Photocatalytic activities

Photocatalytic reactions on Ag-TiO<sub>2</sub> surface can be expressed by the Langmuir–Hinshelwood model [27, 28]. The reaction rate after the adsorption equilibrium can be given as:

$$- \ln (C / C_0) = kt$$

where  $C$  and  $C_0$  are the reactant concentration at time  $t = t$  and  $t = 0$ , respectively;  $k$  and  $t$  are the apparent reaction rate constant and time, respectively. A plot of  $\ln(C / C_0)$  versus  $t$  will yield a slope of  $k$ . Fig. 4 shows the spectral changes of MO in the TiO<sub>2</sub> nanosol, at 0.1.% Ag–TiO<sub>2</sub> nanosol and at 0.5 % Ag–TiO<sub>2</sub> under UV-visible light irradiation. Compared to the pure TiO<sub>2</sub>, the Ag–TiO<sub>2</sub> nanosol exhibited a significant increase in the MO photodegradation rate as shown in Figs. 5.

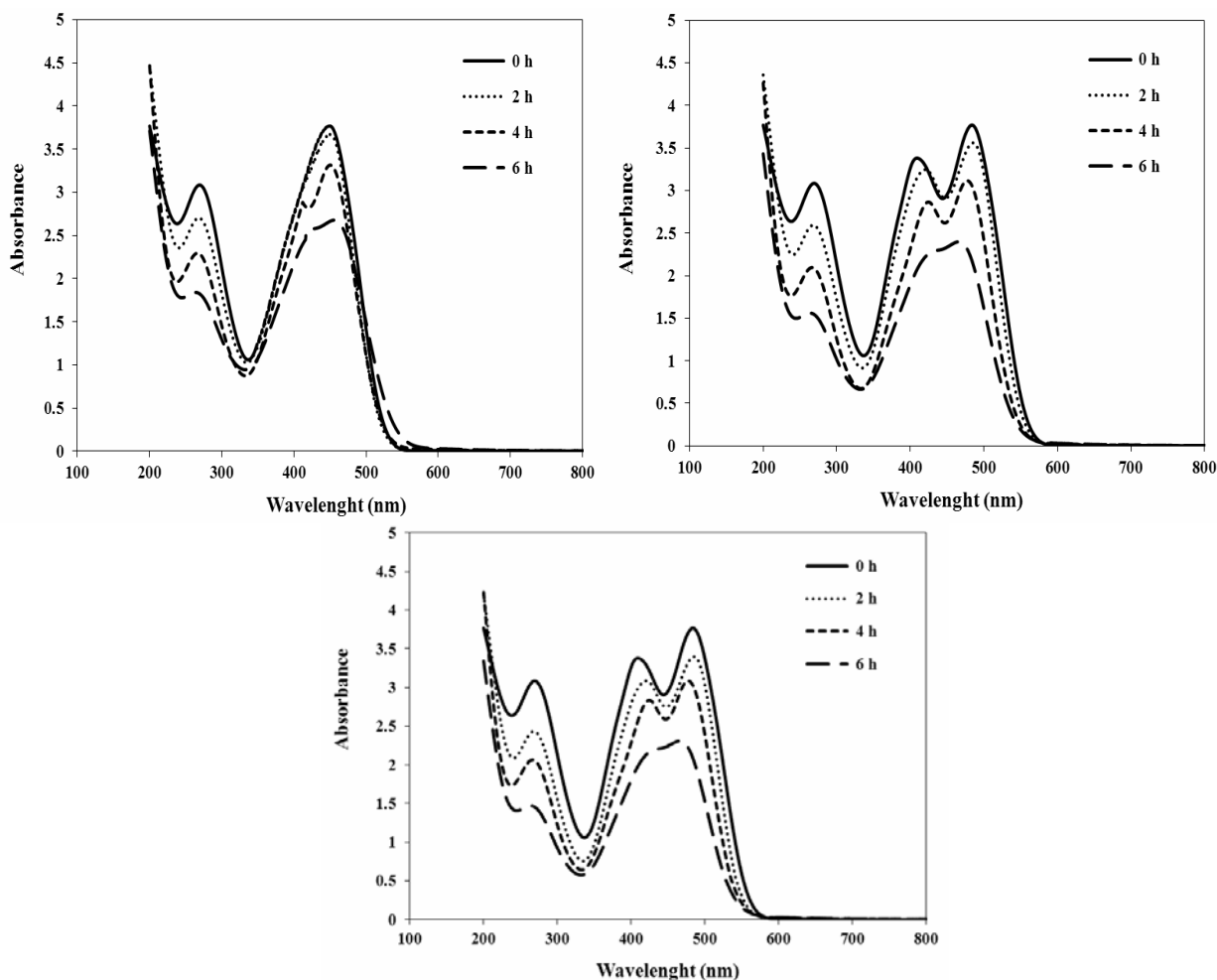


**Fig. 4.** Absorption spectral changes of MO in the (a) TiO<sub>2</sub> nanosol and, (b) at 0.1.% Ag–TiO<sub>2</sub> nanosol, (c) at 0.5.% Ag–TiO<sub>2</sub> nanosol as a function of irradiation time (UV light). The initial concentration ( $C_0$ ) of MO was  $1 \times 10^{-5}$  M, and the TiO<sub>2</sub> content was 0.4 % wt.

The calculated reaction rate constant for the samples prepared with TiO<sub>2</sub> nanosol, at 0.1 % Ag–TiO<sub>2</sub> nanosol and at 0.5 % Ag–TiO<sub>2</sub> were 0.0454, 0.0526 and 0.0625 h<sup>-1</sup>, respectively. However, adding Ag to TiO<sub>2</sub> caused photocatalytic activity to be improved.

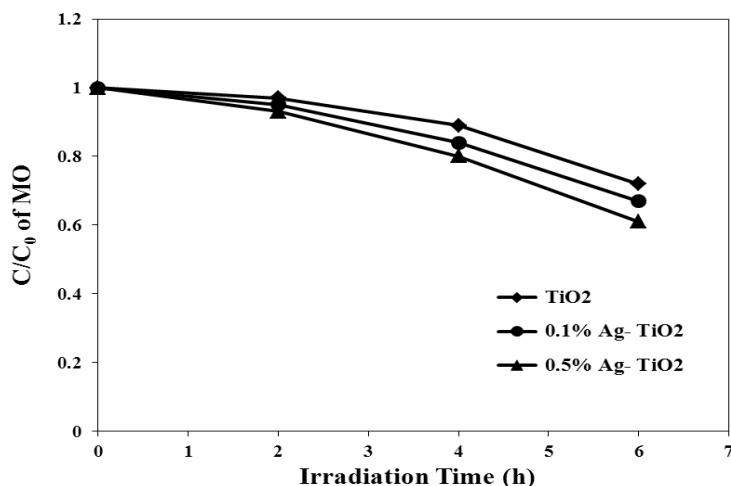


**Fig. 5.** Comparison of the MO photodegradation in the TiO<sub>2</sub>, at 0.1% Ag-TiO<sub>2</sub> and at 0.5% Ag-TiO<sub>2</sub> nanosols under UV light irradiation.

### 3.4. Antibacterial test

To evaluate the antibacterial activity of synthesized materials, 1% weight solution of TiO<sub>2</sub>, 0.1% Ag-TiO<sub>2</sub>, and 0.5% Ag-TiO<sub>2</sub> powders were put upon disks. In this test, a lot of important parameters can be considered. During the performance of test for various samples, we should assimilate parameters such as growing conditions (i.e. time, temperature, and pressure), used culture medium, and amount of cultured bacteria. The results of the antibacterial activity tests of 0.1% and 0.5% silver-deposited titania powders against *E. coli* is presented in Fig.6. It can be seen that the zone of inhibition for 0.5% Ag-TiO<sub>2</sub> is more than that of in 0.1% Ag-TiO<sub>2</sub>.

## 4. CONCLUSION

The Ag-TiO<sub>2</sub> nanoparticles by a high current electrical arc discharge of Ag electrodes have been prepared. XRD results confirm the formation of a mixture of nanocrystalline TiO<sub>2</sub> in rutile phase with silver metals. SEM images demonstrate that the size of Ag-TiO<sub>2</sub> nanoparticles at 5 min arc duration at 50A arc current, are smaller than 1 min arc duration. Photocatalytic activity of TiO<sub>2</sub> and Ag-TiO<sub>2</sub> nanoparticles was measured by photodegradation of MO under 2 mW/cm<sup>2</sup> UV irradiation. The results show that by increasing the irradiation time, both the maximum absorption peak and the concentration of MO decreases. Also it is seen that the photonic efficiency increases with an increase in the metal loading up to an optimum level due to the decreasing of recombination effect of electron and hole. The results of the antibacterial test indicate that the TiO<sub>2</sub> powders itself doesn't exhibit any antibacterial activity against *E. coli*, but the antibacterial activity of powders improves with the addition of the silver metal.

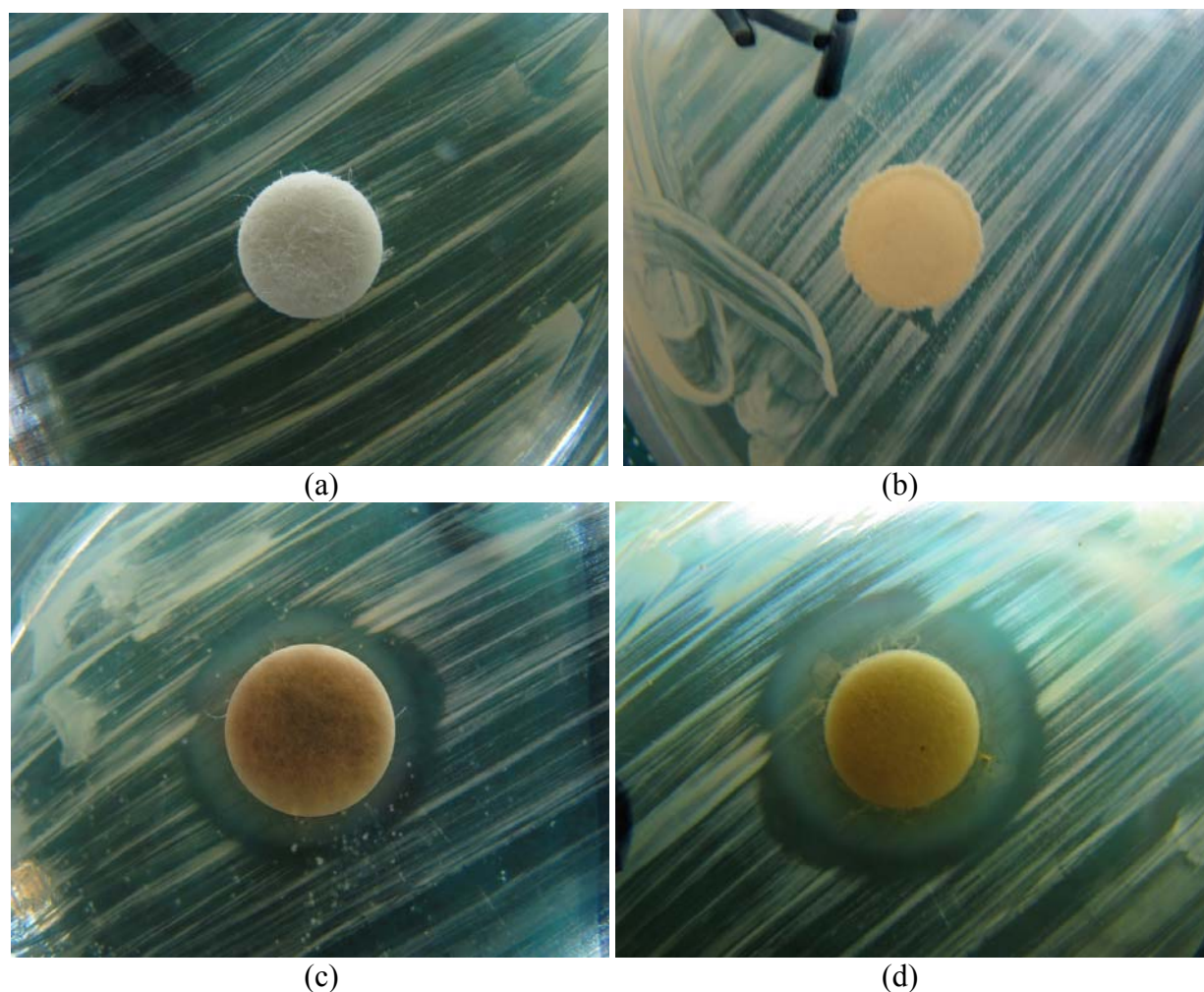


**Fig. 6.** Test results on *E. coli* after 24 h: (a) blank disc, (b) incubated with  $\text{TiO}_2$  film, (c) incubated with 0.1 %Ag- $\text{TiO}_2$  film, (d) incubated with 0.5%Ag- $\text{TiO}_2$  film.

#### ACKNOWLEDGEMENT

The authors are thankful to the research affairs of Bu-Ali Sina University for their financial support of this work. Also, the first author would like to thank to Prof. A.A. Rafati for his valuable discussions during the preparation of this work.

#### REFERENCES

- [1] J. Yu, J. Xiong, B. Cheng, S. Liu, *Appl. Catal. B: Environ.* 60 (2005) 211-221.
- [2] H. Xing-Gang, L. An-Dong, H. Mei-Dong, L. Bin, W. Xiao-Ling, *Chin. Phys. Lett.* 26 (2009) 771061-771064.
- [3] L. Escobar-Alarco'n, A. Arrieta, E. Camps, S. Muhl, S. Rodil, E. Viguera-Santiago, *Appl. Surf. Sci.* 254 (2007) 412-415.
- [4] C.C. Chang, J.Y. Chen, T.L. Hsu, C.K. Lin, C.C. Chan, *Thin Solid Films* 516 (2008) 1743-1747.
- [5] L. Wan, J.F. Li, J.Y. Feng, W. Sun, Z.Q. Mao, *Mater. Sci. Eng. B* 139 (2007) 216-220.
- [6] J. McCormick, B. Zhao, S. Rykov, H. Wang, J.G. Chen, *J. Phys. Chem. B* 108 (2004) 17398-17402.
- [7] L. Zan, L. Tian, Z. Liu, Z. Peng, *Appl. Catal. A Gen.* 264 (2004) 237-242.
- [8] B. Xin, Z. Ren, H. Hu, X. Zhang, C. Dong, K. Shi, L. Jing, H. Fu, *Appl. Surf. Sci.* 252 (2005) 2050-2055.
- [9] L. Ge, M. Xu, H. Fang, *J. Mol. Catal. A-Chem.* 258 (2006) 68-76.
- [10] M. Hemissi, H. Amardjia-Adnani, J. Plenet, *Curr. Appl. Phys.* 9 (2009) 717-721.
- [11] S. Sekhar Samal, P. Jeyaraman, V. Vishwakarma, *J. Min. Mater. Char. Eng.* 9 (2010) 519-525.
- [12] M. Nasr-Esfahani, H. Habibi, *Int. J. Photoenergy* (2008) Article ID 628713.

- [13] C. Li, Y. Hsieh, W. Chiu, C. Liu, C. Kao, *Sep. Purif. Technol.* 58 (2007) 148-151.
- [14] M. Lee, S. Hong, M. Mohseni, *J. Mol. Catal. A-Chem.* 242 (2005) 135-140.
- [15] J. Matos, J. Laine, J. Herrmann, *Appl. Catal. B-Environ.* 18 (1998) 281-291.
- [16] S. Sena, S. Mahanty, S. Roy, O. Heintz, S. Bourgeois, D. Chaumont, *Thin Solid Films* 474 (2005) 245-249.
- [17] L. Ren, Y. Zeng, D. Jiang, *Catal. Commun.* 10 (2009) 645-649.
- [18] H. Sung-Suh, J. Choi, H. Hah, S. Koo, Y. Bae, *J. Photochem. Photobio. A* 163 (2004) 37-44.
- [19] S. Sun, B. Sun, W. Zhang, D. Wang, *Bull. Mater. Sci.* 31 (2008) 61-66.
- [20] C. Li-yuan, W. Shun-wen, P. Bing, L. Zhu-ying, *Trans Nonferrous met. Soc. China* 18 (2009) 980-985.
- [21] X. Houa, M. Huanga, X. Wub, A. Liu, *Chem. Eng. J.* 146 (2009) 42-48.
- [22] J. Sung Kim, S. Jin Park, Y. Kyung Park, C. Hwang, *Nanomed. Nanotechnol. Biol. Med.* 3 (2007) 95-101.
- [23] X. Chen, H. Schluesener, *Toxicol. Lett.* 176 (2008) 1-12.
- [24] A. Ashkarran, *Curr. Appl. Phys.* 10 (2010) 1442-1447.
- [25] W. Lawrence Drew, A.L. Barry, R. Otoole, J.C. Sherris, *Appl. Environ. Microbiol.* 24(2) (1972) 240-247.
- [26] B. Ghalem, B. Mohamed, *African J. Pharm. Pharmaco.* 3 (2009) 92-96.
- [27] D. Liao, C. Badour, B. Liao, *J. Photochem. Photobio. A* 194 (2008) 11-19.
- [28] Y. Li, X. Li, J. Li, J. Yin, *Water Res.* 40 (2006) 1119-1126.